Electronic Supplementary Material (ESI) for ChemComm.

SUPPORTING INFORMATION

Design of high-avidity multivalent ligand structures that target cells with high ligand economy

Qingqing Fang, Pan Guo, Yiting Zeng, Chenru Wang, Tao Jiang* and Yunbao Jiang*

Table of Contents

1. Materials
2. Syntheses and preparations of the ligand structures
3. Sequences of the peptides and the oligonucleotides
4. Experimental methods
5. Supplementary data
6. References

1. Materials

Fmoc-N-amino acids for peptide syntheses were purchased from GL Biochem., Ltd. bis(maleimido)triethylene glycol was purchased from Thermo Scientific, Inc. FITC and chemicals for synthesis of sugar derivatives were purchased from Shanghai Bide Pharm., Ltd. Cell-tracker red CMTPX was purchased from Maokang Biotechnology Co. Ltd. Hoechst 33342, DiI and the oligonucleotides of AS1411 and GT31 were purchased from Sangon Biotech (Shanghai, China) and used without further purification. All reagents and solvents used in synthesis were commercially available at analytical grade or higher. Water was Milli-Q-grade water (18.2 MΩ cm).

2. Syntheses and preparations of the ligand structures

Syntheses of the peptides

The coiled-coil and sheet-forming peptides were synthesized on a CEM Liberty solid-phase synthesizer. For the FITC-labeled peptides, the protected peptides on the resins were incubated with FITC (5 eq.) and DIEA (2 eq.) in DMF overnight at 37℃. The resulting peptides were cleaved from the resins using the cleavage cocktails (for thiol-containing peptides, using 91% TFA, 3.0% TIPS, 3.0% EDT and 3.0% water; for others, using 95% TFA, 2.5% TIPS, 2.5% water). For the fluorescein (FAM)-labeled peptides, the purified thiol-containing peptides were incubated with fluorescein-5-maleimide (1.5 eq.) and TCEP (0.2 eq.) at 25 °C for 5 h. All final peptides and dye-labelled derivatives were purified via RP-HPLC on a C18 column with a gradient of water-acetonitrile with 0.1% TFA. The target fractions were lyophilized and stored at 4℃.

Synthesis of the unnatural amino acids and ligands

Fmoc-Lys[N-4-pentynoic acid]-OH:

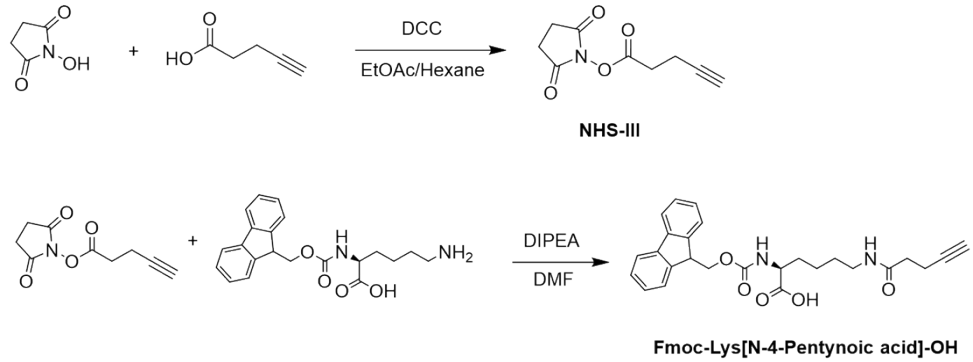

Scheme S1. Synthesis route of **Fmoc-Lys[N-4-pentynoic acid]-OH**.

As shown in Scheme S1, **NHS-III** and **Fmoc-Lys[N-4-pentynoic acid]-OH** were synthesized following the reported procedures[1], as white solids with the yield of 97% and 91%, respectively.

NHS-III: ^{1}H NMR (500 MHz, $CDCl_3$): δ 2.88 (dd, J = 8.1, 6.8 Hz, 2H), 2.84 (s, 4H), 2.62 (ddd, J = 8.6, 6.8, 2.7 Hz, 2H), 2.06 (t, J = 2.7 Hz, 1H). ^{13}C NMR (126 MHz, $CDCl_3$): δ 168.95, 167.03, 80.88, 70.05, 30.29, 25.58, 14.08. HRMS (ESI): calcd. for $C_9H_9NO_4$: $[M+Na]^+$ 218.0424, found 218.0429.

Fmoc-Lys[N-4-pentynoic acid]-OH: ^{1}H NMR (500 MHz, $CDCl_3$): δ 7.75 (d, *J* = 7.5 Hz, 2H), 7.60 (t, *J* = 8.1 Hz, 2H), 7.39 (t, *J* = 7.5 Hz, 2H), 7.30 (t, *J* = 7.5 Hz, 2H), 6.03 (s, 1H), 5.73 (d, *J* = 7.9 Hz, 1H), 4.52–4.32 (m, 3H), 4.20 (t, *J* = 7.1 Hz, 1H), 3.35–3.22 (m, 2H), 2.52–2.48 (m, 2H), 2.39 (t, *J* = 7.0 Hz, 2H), 2.00 (s, 1H), 1.95–1.85 (m, 1H), 1.82–1.72 (m, 1H), 1.55 (dd, *J* = 13.6, 6.7 Hz, 2H), 1.50–1.24 (m, 3H). ^{13}C NMR (126 MHz, $CDCl_3$): δ 174.84, 172.05–171.92, 143.70, 141.29, 127.74, 127.11, 125.13, 120.00, 82.74, 69.78, 67.12, 53.49, 47.13, 39.13, 35.26, 31.73, 28.85, 22.07, 15.01. HRMS (ESI): calcd. for $C_{26}H_{28}N_2O_5$: $[M+Na]^+$ 471.1890, found 471.1898.

Fmoc-Lys-S-Trt:

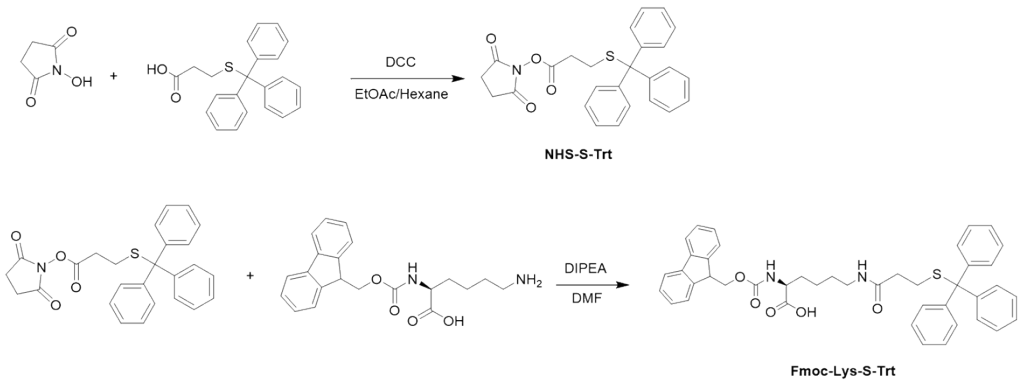

Scheme S2 Synthesis route of **Fmoc-Lys-S-Trt**.

As shown in Scheme S2, **NHS-S-Trt** and **Fmoc-Lys-S-Trt** were synthesized following the reported procedures[2] with the yield of 100% and 85%, respectively.

NHS-S-Trt: ^{1}H NMR (500 MHz, $CDCl_3$): δ 7.44 (d, *J* = 7.5 Hz, 6H), 7.30 (t, *J* = 7.7 Hz, 6H), 7.22 (t, *J* = 7.3 Hz, 3H), 2.80 (s, 4H), 2.55 (t, *J* = 7.5 Hz, 2H), 2.40 (t, *J* = 7.5 Hz, 2H). ^{13}C NMR (126 MHz, $CDCl_3$): δ 168.85, 167.06, 144.33, 129.52, 128.06, 126.84, 67.14, 30.50, 26.09, 25.54. HRMS (ESI): calcd. for $C_{26}H_{23}NO_4S$: $[M+Na]^+$ 468.1240, found 468.1241.

Fmoc-Lys-S-Trt: ^{1}H NMR (500 MHz, DMSO-d_6): δ 12.55 (s, 1H), 7.89 (d, *J* = 7.5 Hz, 2H), 7.80 (t, *J* = 5.1 Hz, 1H), 7.72 (d, *J* = 7.4 Hz, 2H), 7.62 (d, *J* = 7.9 Hz, 1H), 7.41 (t, *J* = 7.0 Hz, 2H), 7.34 – 7.29 (m, 15H), 7.24 (d, *J* = 6.7 Hz, 2H), 4.27 (t, *J* = 8.5 Hz, 2H), 4.22 (t, *J* = 7.0 Hz, 1H), 3.92 – 3.88 (m, 1H), 2.99 (s, 2H), 2.23 (t, *J* = 7.2 Hz, 2H), 2.13 (t, *J* = 7.2 Hz, 2H), 1.68 (s, 1H), 1.59 (s, 1H), 1.35 (s, 4H). ^{13}C NMR (126 MHz, DMSO-d_6): δ 173.89, 169.68, 156.06, 144.34, 143.71, 140.61, 128.96, 127.90, 127.53, 126.96, 126.58, 125.18, 120.02, 65.84, 65.48, 53.62, 46.55, 39.76, 39.55, 39.41, 39.30, 39.27, 39.13, 38.99, 38.16, 33.89, 30.27, 28.47, 27.40, 22.93. HRMS (ESI): calcd. for $C_{43}H_{42}N_2O_5S$: $[M+Na]^+$ 721.2707, found 721.2706.

Azide-mannose:

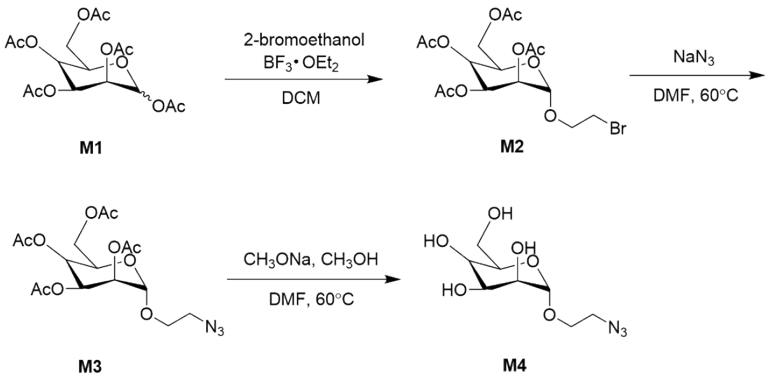

Scheme S3. Synthesis route of **azide-mannose**.

As shown in Scheme S3, the mannose derivatives were synthesized following the reported procedures[3] with the yield of **M2** at 82% yield, **M3** at 98%, and **M4** at 89%.
M2: ^{1}H NMR (500 MHz, $CDCl_3$): δ 5.35 (dd, *J* = 10.1, 3.4 Hz, 1H), 5.31–5.29 (m, 1H), 5.28–5.27 (m, 1H), 4.88 (d, *J* = 1.7 Hz, 1H), 4.28 (dd, *J* = 12.7, 6.0 Hz, 1H), 4.16–4.12 (m, 2H), 3.98 (dt, *J* = 11.2, 6.3 Hz, 1H), 3.89 (dt, *J* = 11.3, 5.7 Hz, 1H), 3.52 (t, *J* = 6.0 Hz, 2H), 2.16 (s, 3H), 2.11 (s, 3H), 2.06 (s, 3H), 2.00 (s, 3H). ^{13}C NMR (126 MHz, $CDCl_3$): δ 170.66, 170.05, 169.83, 97.79, 69.42, 68.90, 67.10, 66.04, 62.50, 50.40, 20.79. HRMS (ESI): calcd. for $C_{16}H_{23}BrO_{10}$: $[M+Na]^+$ 479.0349, found 479.0352.
M3: ^{1}H NMR (500 MHz, $CDCl_3$): δ 5.37 (dd, J = 10.0, 3.4 Hz, 1H), 5.30 (s, 1H), 5.28 (dd, J = 3.2, 1.9 Hz, 1H), 4.87 (d, J = 1.5 Hz, 1H), 4.29 (dd, J = 12.3, 5.3 Hz, 1H), 4.13 (dd, J = 12.3, 2.4 Hz, 1H), 4.05 (ddd, J = 9.7, 5.3, 2.3 Hz, 1H), 3.90–3.85 (m, 1H), 3.70–3.65 (m, 1H), 3.52–3.42 (m, 2H), 2.16 (s, 3H), 2.11 (s, 3H), 2.05 (s, 3H), 2.00 (s, 3H). ^{13}C NMR (126 MHz, $CDCl_3$): δ 170.66, 170.05, 169.83, 97.79, 69.42, 68.90, 67.10, 66.04, 62.50, 50.40, 20.79. HRMS (ESI): calcd. for $C_{16}H_{23}N_3O_{10}$: $[M+Na]^+$ 440.1276, found 440.1285.
M4: ^{1}H NMR (500 MHz, DMSO-d_6): δ 4.76 (s, 2H), 4.68 (d, J = 1.1 Hz, 1H), 4.60 (s, 1H), 4.47 (s, 1H), 3.78 (ddd, J = 10.2, 6.5, 3.4 Hz, 1H), 3.69–3.61 (m, 2H), 3.58–3.53 (m, 1H), 3.50– 3.35 (m, 6H). ^{13}C NMR (126 MHz, DMSO-d_6): δ 99.97, 74.18, 70.79, 70.18, 66.89, 65.61, 61.25, 49.98. HRMS (ESI): calcd. for $C_8H_{15}N_3O_6$: $[M+Na]^+$ 272.0853, found 272.0855.

Preparations of the ligand-peptide conjugates
Mannose-peptide conjugates (P1-Man, **P2-Man** and **P1-2-Man**, **P2-2-Man):** the FITC labelled, alkyne-containing **P1** or **P2** peptides in PBS (100 mM, pH = 7.4) with 6 M guanidine hydrochloride were mixed with **M4** (3 eq.), THPTA (3 eq.), $CuSO_4$ (5 eq.), and sodium ascorbate (100 eq.), for a 12 h incubation in N_2 atmosphere at room temperature. **P1-2-Man** and **P2-2-Man** were synthesized in a similar way except for doubling the amount of **M4**, THPTA and $CuSO_4$. The peptides were treated with TCEP (0.2 eq.) to prevent disulfide formation right before the click reactions.

NSI*-P2*-Man and **NSI*-P2*-2-Man:** As shown in Scheme S4, **P2*-Man** or **P2*-2-**

Man was incubated with bis(maleimido)triethylene glycol (5 eq.) at room temperature for 4 h to obtain Mal-PEG$_3$-P2*-Man or Mal-PEG$_3$-P2*-2-Man, respectively. The HPLC purified conjugate was then mixed with the sheet-forming peptide **NSI*** (1 eq.) at room temperature for 12 h to form the final conjugates.

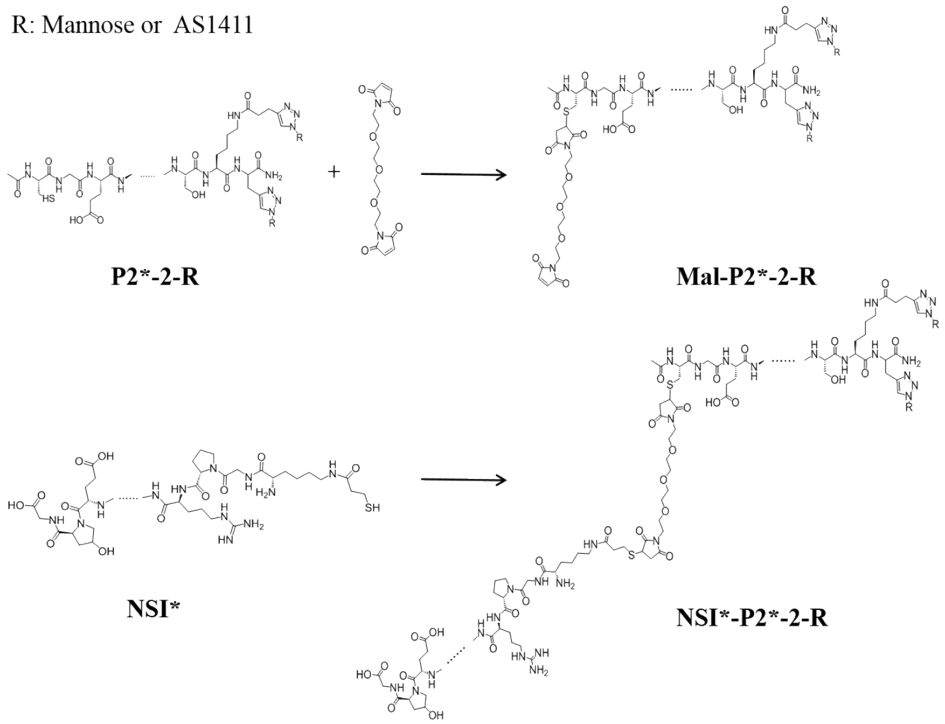

Scheme S4. Synthesis route of **NSI*-P2*-2-R**.

Aptamer-peptide conjugates (FITC-P1-AS1411, **P2-AS1411** and **P2-2-AS1411):** Commercially available amine-modified **AS1411** in PB buffer was mixed with **DBCO-NHS** (50 eq.) in DMSO (3:1, volume ratio) overnight at 50℃. The resultant **AS1411-DBCO** was purified through the spin-filtration (dialysis membrane MWCO = 3,500 Da). **FITC-P1-AS1411**, **P2-AS1411** and **P2-2-AS1411** were prepared through the copper-free click reactions by mixing **AS1411-DBCO** with **FITC-P1-N$_3$**, **P2-N$_3$** and **P2-2-N$_3$** (2 eq.) in the presence of 5 mM aminoguanidine hydrochloride, overnight at 50℃, respectively. **NSI*-P2*-AS1411** and **NSI*-P2*-2-AS1411** were prepared

Preparation of the multivalent ligand structures

Ligand clusters: the mono-, di-, and tri-ligand clusters were prepared through the equimolar mixing of the corresponding P1, P2 with or without the ligands in PBS at room temperature.

Peptide nanosheets and ligand-nanosheet conjugates: sheet-forming peptides **NSI** and the ligand conjugated peptides (**NSI*-P2*-Man**, **NSI*-P2*-2-Man**, **NSI*-P2*-AS1411** and **NSI*-P2*-2-AS1411**) were dialyzed against water thoroughly to remove residual TFA (dialysis membrane MWCO = 2,000 Da). Using a water bath, the peptide mixtures in MOPS buffer (20 mM, pH = 7.0) were subjected to a thermal

annealing to facilitate the nanosheet formation using the following procedure: 75℃ 45 min, and then cool down to 26℃ over 12 h. The corresponding **P1** peptides with or without the ligands (1 eq. to the **P2** in the nanosheets) were added to the annealed samples to form the final multivalent ligand structures. The samples turn cloudy upon the nanosheet formation. The supernatant buffer was exchanged to PBS to "wash" the ligand structures through sample centrifugations. The annealed samples were stored at 26℃ prior to measurements.

3. Sequences of the peptides and the oligonucleotides

FITC-P1: FITC-(β-Ala)-GKIQQLKQKIQALKEENAALEYENAQLEQ-amide
P2-1: Ac-GEIAALEEEIAQLEQKNQQLKYKNQALKEGGS Pra-amide
FITC-P1-1: FITC-(β-Ala)-GKIQQLKQKIQALKEENAALEYENAQLEQGGS Pra-amide
P2-2: Ac-GEIAALEEEIAQLEQKNQQLKYKNQALKEGGS Lys(III) Pra-amide
P2*-2: Ac-CGEIAALEEEIAQLEQKNQQLKYKNQALKEGGS Lys(III) Pra-amide
FITC-P1-N_3: FITC-(β-Ala)-GKIQQLKQKIQALKEENAALEYENAQLEQGGS Lys(N_3)-amide
P2-N_3: Ac-GEIAALEEEIAQLEQKNQQLKYKNQALKEGGS Lys(N_3)-amide
P2-2-N_3: Ac-GEIAALEEEIAQLEQKNQQLKYKNQALKEGGS Lys(N_3) Lys(N_3)-amide
P2*-N_3: Ac-CGEIAALEEEIAQLEQKNQQLKYKNQALKEGGS Lys(N_3)-amide
P2*-2-N_3: Ac-CGEIAALEEEIAQLEQKNQQLKYKNQALKEGGS Lys(N_3) Lys(N_3)-amide
NSI: NH_2-$(PRG)_4$-$(POG)_4$-$(EOG)_4$-COOH
NSI*: NH_2-Lys(SH)-G-$(PRG)_4$-$(POG)_4$-$(EOG)_4$-COOH
AS1411: NH_2-C6-TTTTTGGTGGTGGTGGTTGTGGTGGTGGTGG-3'
GT31: 5'-GTTGTTGTTTGGTGTGGGTTTGGGGTGTGGG-3'
Pra denotes propargylglycine, Lys(III) denotes Lys[N-4-pentynoic acid]-OH, Lys(N_3) denotes (2S)-N-5-azido-hexanoic acid, O denotes 4-hydroxy-proline. Ac means acetyl group.

4. Experimental methods

Circular dichroism spectropolarimetry

CD measurements were performed on a Jasco J-1500 spectropolarimeter using 0.10 mm quartz cell. Spectra were recorded from 260 nm to 190 nm at a scanning rate of 100 nm/min and a resolution of 1 nm. CD melting experiments were performed from 4℃ to 85℃ at a heating rate of 1℃/min and the intensity of the CD signal at 222 nm was monitored.

Size exclusion chromatography

SEC spectra of the samples P1, P2 and P1P2 were acquired on a ÄKTA pure protein purification system using a Superdex peptide 10/300 GL column and PBS as the elution buffer. The peptide signals were monitored at 280 nm.

Transmission electron microscopy

TEM images were obtained on a JEM-1400 transmission electron microscope at an accelerating voltage of 100 kV. The peptide samples were deposited onto a 200-mesh grid (from Electron Microscopy, China), and stained with phosphotungstic acid (as 1%

PTA solution, pH 6.5). The stained specimens were dried under vacuum before the investigations.

Dynamic light scattering

DLS measurements of FITC-labelled P1-P2 coiled coil, the NSI nanosheet, and the sheet modified with the coiled coils were performed on a Malvern Zetasizer Nano instrument, equipped with a 4 mW, He-Ne laser with an emission wavelength at 633 nm. The samples were diluted with PBS buffer to afford the proper scattering intensities for the instrument, and equilibrated for 30 s prior to data acquisition. The data were automatically modelled using a sphere particle model to give the reported hydrodynamic diameters.

Cell culture

MDA-MB-231 cells were maintained in a high-glucose DMEM medium, supplemented with 10% FBS and 1% penicillin/streptomycin (penicillin, 10,000 U/mL; streptomycin, 10,000 U/mL) at 37°C in a humidified atmosphere containing 5% CO_2. The cells were passaged at about 80% cell confluency using a 0.25% trypsin solution.

Fluorescence confocal microscopy

The cells for imaging were seeded in culture plates (1.0×10^5 cells/plate) and incubated for 24 h at 37°C, 5% CO_2. After medium removal, the cells were immediately incubated with the ligand structures in 500 μL PBS at 37°C for 2 h. After cell washing using PBS, Hoechst 33342 was added to stain the DNA for 5 min at 37°C. After cell washing using PBS, DiI was added to label cell membranes for 10 min. The confocal images of the resultant specimens were acquired from a Leica TCS SP8 microscope, with a Leica 63 × oil-immersion objective (numerical aperture, NA 1.4). The fluorophores Hoechst, FITC and DiI were excited at 405 nm, 488 nm, and 552 nm, respectively. The images were obtained using sequential scanning mode, using 425-478 nm, 505-555 nm, and 565-652 nm bands, respectively.

In order to evaluate the effect of potential cellular uptake of the ligand structures, the confocal imaging was performed for the cells labelled with a lysosome-specific dye (Lyso-Tracker Red) and Hoechst 33342. These dye-labelled cells were incubated with the multivalent tri-mannose and tri-AS1411 clusters on the nanosheets for 2 h at 5°C and 37°C, respectively, as cellular uptakes should be suppressed at 5°C compared with that at 37°C.

Flow cytometry

The cells were seeded in 24-well plates (1.5×10^5 cells/well) and incubated for 24 h at 37°C, 5% CO_2. After medium removal, the cells were incubated with the ligand structures of varied concentrations in 500 μL PBS at 37°C for 2 h. The ligand-bound cells were resuspended using PBS and then subject to flow cytometry measurements by tracking the signals of the FITC appended to the ligands from BD FACS Aria II flow cytometry. 10,000 live cell events were collected for each analysis.

Two competitive binding assays were conducted using flow cytometry. 1st sample: The cells were incubated with 5 μM FITC-labelled mono-mannose with 0, 5, 10, and 25 μM di-mannose clusters without the fluorophore, respectively. 2nd sample: The cells were incubated with 5 μM FITC-labelled di-mannose clusters with 0 and 25 μM unlabeled mono-mannose, respectively.

Estimation of the amount of the cell-surface mannose receptors (MRs) and nucleolin protein

As indicated in Fig. 3, the FITC intensities of the ligand-cell samples reached a plateau at 200 μM mono-mannose and 350 nM mono-AS1411 ligand structures, respectively. 1.5×10^5 MDA-MB-231 cells were tested in each specimen with a total volume of 500 μL. Assuming one mono-ligand binds to one cell-surface receptor, the average amount of the MRs and nucleolin proteins was estimated to be 4.0×10^{11} and 7.0×10^8/cell, respectively. The calculated values represent the upper limit of the receptor number, considering the scenario that single receptor associates with multiple ligands.

5. Supplementary data

Table S1. Mass data of the peptides and the ligand-peptide conjugates

Compound	Chemical formula$(M+H)^+$	MALDI$(M+H)^+$	
		Cald.	Found
FITC-P1	$C_{170}H_{260}N_{44}O_{54}S$	3815.87	3815.79
P2-1	$C_{160}H_{261}N_{45}O_{55}$	3694.91	3695.03
FITC-P1-1	$C_{182}H_{276}N_{48}O_{59}S$	4111.98	4112.06
P2-2	$C_{171}H_{277}N_{47}O_{57}$	3903.03	3903.11
P2*-2	$C_{174}H_{282}N_{48}O_{58}S$	4006.04	4006.06
P1*-1	$C_{163}H_{267}N_{55}O_{55}S$	3795.93	3795.86
FITC-P1-N_3	$C_{183}H_{281}N_{51}O_{59}S$	4171.03	4171.10
P2-N_3	$C_{161}H_{266}N_{48}O_{55}$	3753.95	3753.06
P2*-N_3	$C_{164}H_{271}N_{49}O_{56}S$	3856.96	3856.26
P2-2-N_3	$C_{167}H_{276}N_{52}O_{56}$	3908.04	3908.84
P2*-2-N_3	$C_{170}H_{281}N_{53}O_{57}S$	4011.05	4010.98
NSI	$C_{148}H_{226}N_{48}O_{53}$	3524.65	3524.83
NSI*	$C_{159}H_{245}N_{51}O_{56}S$	3798.77	3799.05
P2-Man	$C_{168}H_{276}N_{48}O_{61}$	3944.00	3943.95
FITC-P1-Man	$C_{190}H_{291}N_{51}O_{65}S$	4361.08	4360.86
P2-2-Man	$C_{187}H_{307}N_{53}O_{69}$	4401.22	4401.70
P2*-2-Man	$C_{190}H_{312}N_{54}O_{70}S$	4504.23	4505.22
Mal-P2*-2-Man	$C_{206}H_{332}N_{56}O_{77}S$	4856.36	4856.98
P1*-Man	$C_{171}H_{282}N_{50}O_{61}S$	4045.03	4045.21
FAM-P1*-Man	$C_{195}H_{295}N_{51}O_{68}S$	4473.10	4473.18

FAM-P2*-2-Man	$C_{214}H_{325}N_{55}O_{77}S$	4931.30	4931.45
Mal-P2*-N_3	$C_{180}H_{291}N_{51}O_{63}S$	4209.09	4209.64

Compound	Chemical formula$(M+H)^+$	ESI-Q-TOF-MS	
		Cald.	Found
AS1411-DBCO	$C_{335}H_{414}N_{115}O_{203}P_{31}$	$[M+H]^{4+}$ 2564.93	2564.87
FITC-P1-AS1411	$C_{518}H_{695}N_{166}O_{262}P_{31}S$	$[M+H]^{10+}$ 1443.13	1443.22
P2-AS1411	$C_{496}H_{680}N_{163}O_{258}P_{31}$	$[M+H]^{11+}$ 1273.99	1273.96
P2-2-AS1411	$C_{837}H_{1104}N_{282}O_{462}P_{62}$	$[M+H]^{11+}$ 2220.70	2220.64
P2*-2-AS1411	$C_{840}H_{1111}N_{283}O_{459}P_{62}S$	$[M+H]^{11+}$ 2224.42	2224.52
Mal-P2*-2-AS1411	$C_{856}H_{1129}N_{285}O_{470}P_{62}S$	$[M+H]^{14+}$ 1777.37	1777.43

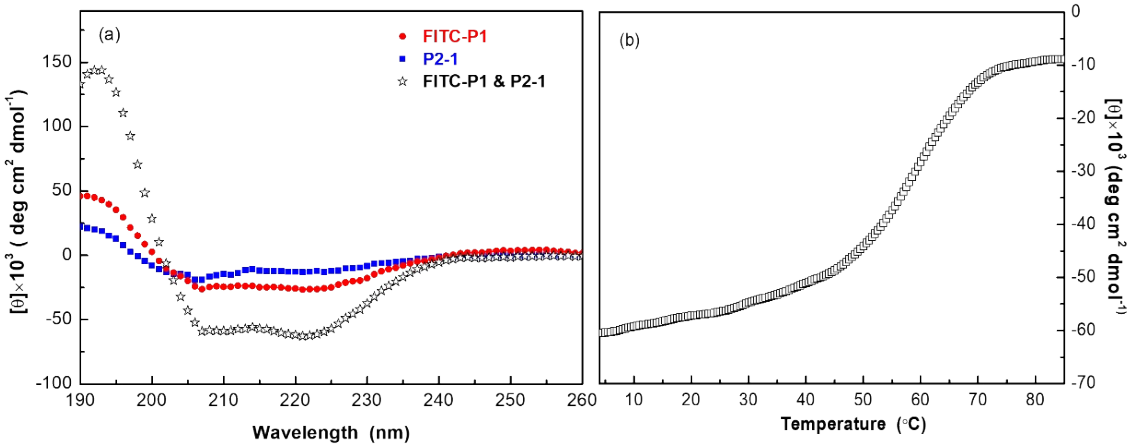

Figure S1. (a) CD spectra of **FITC-P1**, **P2-1** and **FITC-P1** & **P2-1**. (b) Melting curves of **FITC-P1** & **P2-1** in PBS. The concentration of each peptide was 100 μM.

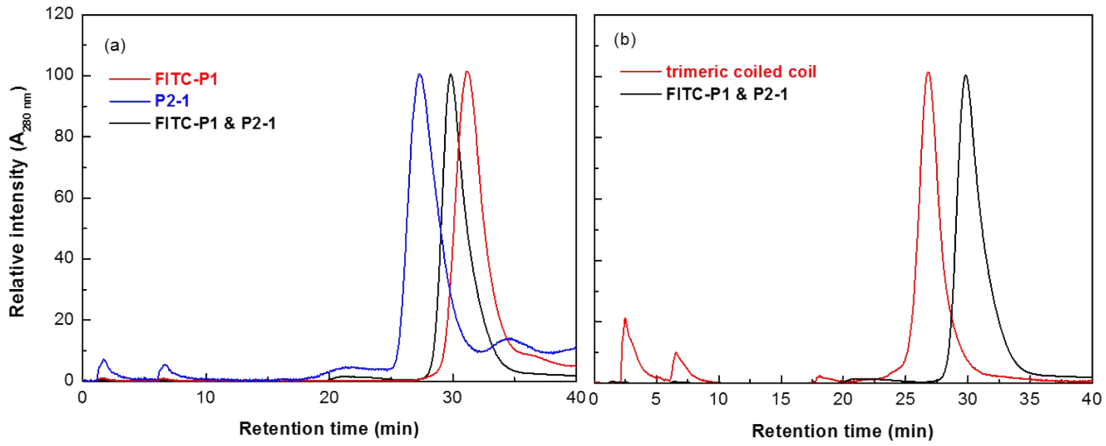

Figure S2. SEC spectra of the coiled-coil peptides. (a) **FITC-P1**, **P2-1** and **FITC-P1** & **P2-1** were eluted at 31.1 min, 27.3 min and 29.8 min, respectively. (b) The trimeric coiled coil structure was used as a control that eluted at 26.8 min (Ac-G EIAAIKK EIAAIK Hcy EIAAIKE EIAAIKQ GY-amide, Hcy denotes homocysteine)

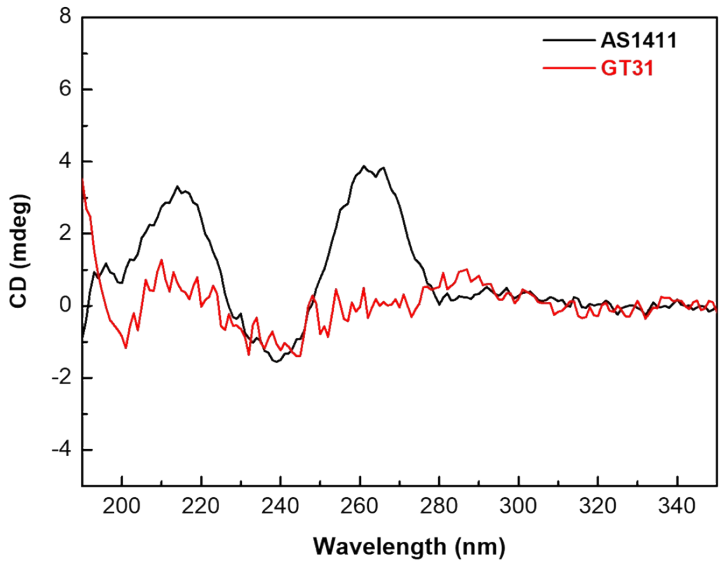

Figure S3. CD spectra of **AS1411** and **GT31** in PBS containing 5.0 mM $MgCl_2$. **GT31** has the same base composition as **AS1411**, with a scrambled sequence.

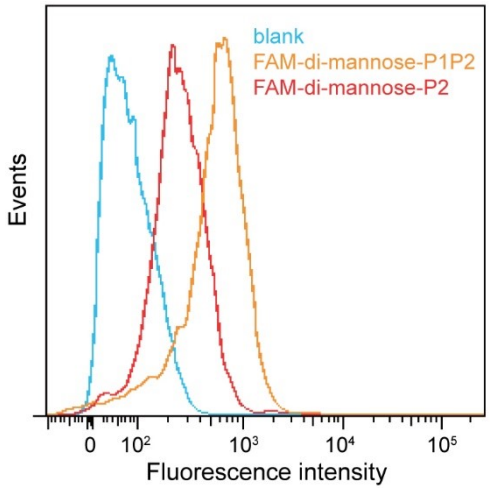

Fig. S4. Flow cytometry analyses of cell-binding performance of the fluorescein-labelled di-mannose clusters on the P1-P2 coiled coil (yellow) and single peptide P2 (red). The sequences of the two types of the ligand-scaffold structures are shown in Fig. 1, using fluorescein instead of FITC this time. Blank denotes the cells without the ligands.

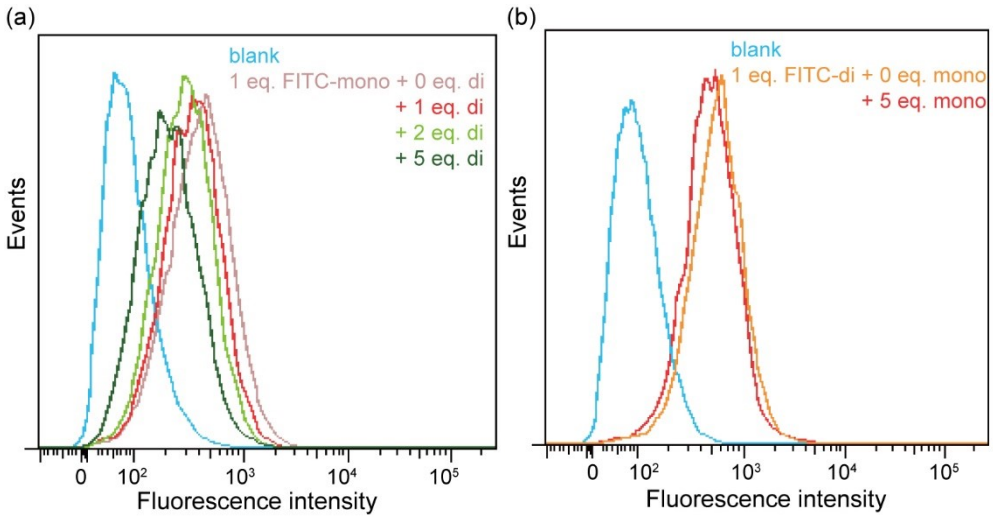

Fig. S5. Competitive binding assays using flow cytometry. (a) The MDA-MB-231 cells were incubated with FITC-labelled mono-mannose ligands with varied amount of unlabeled di-mannose clusters. (b) The cells were incubated with FITC-labelled di-mannose clusters in the presence of excess unlabeled mono-mannose ligands. Blank denotes the cells without the ligands.

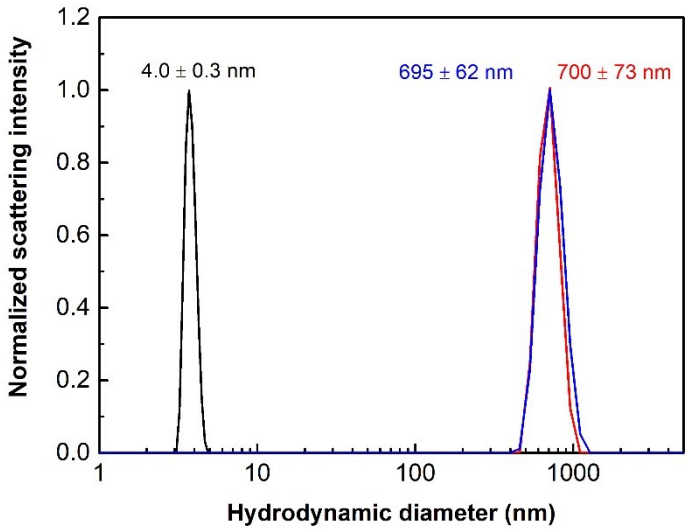

Figure S6. DLS size distributions of **P1-P2** (black), **NSI** nanosheets (blue), and the **NSI** nanosheets doped with **P1-P2** coiled coils (red).

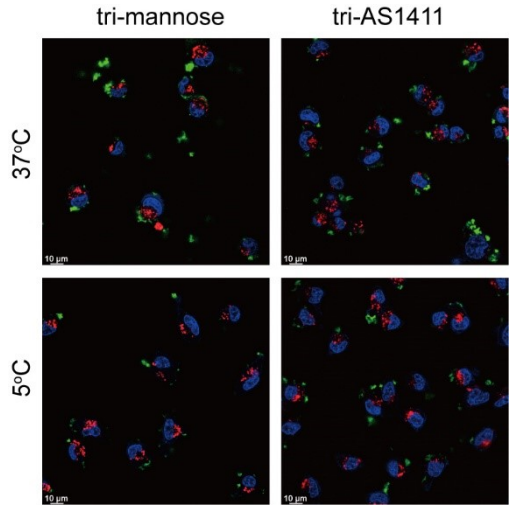

Figure S7. Targeting of the FITC-labelled tri-mannose and tri-AS1411 clusters on the NSI nanosheets to MDA-MB-231 cells at 37℃ and 5℃, respectively. The cells were labelled with the lysosome-specific dye (Lyso-tracker Red, red) and the DNA-specific dye (Hoechst, blue).

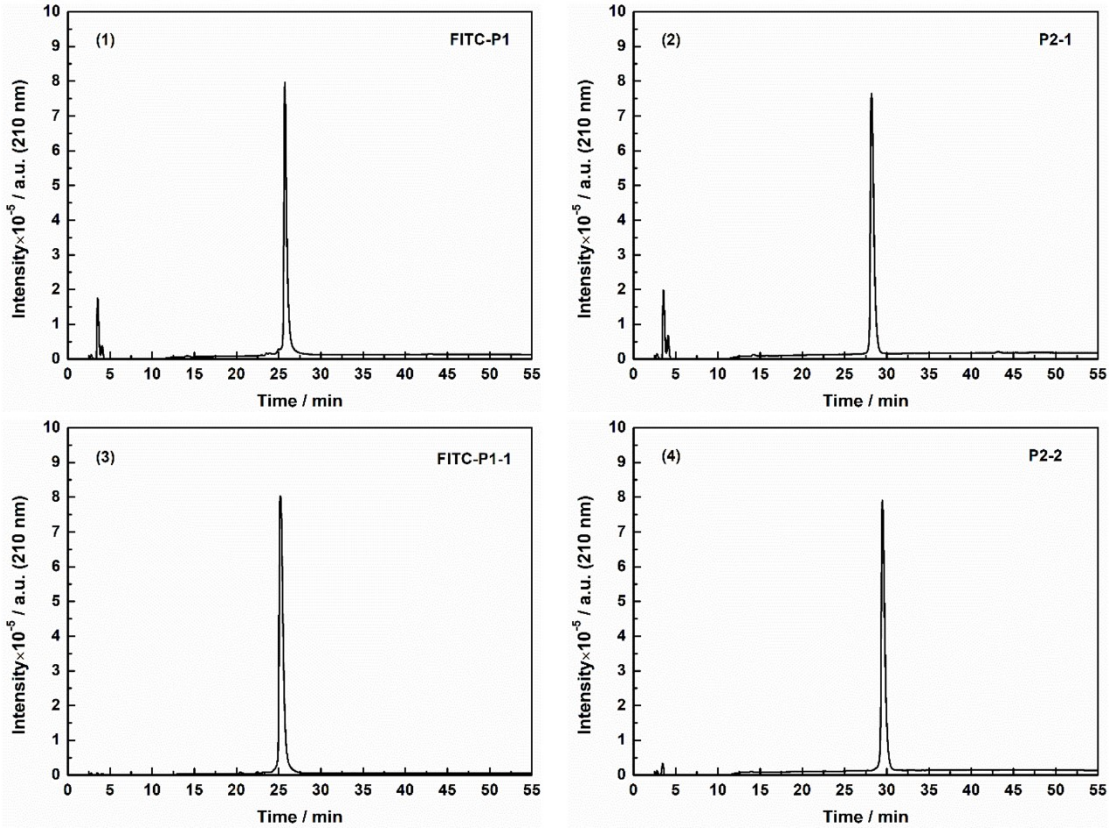

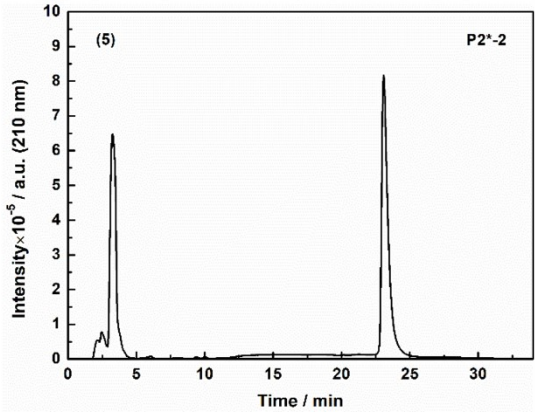
(5)
P2*-2
Intensity×10^{-5} / a.u. (210 nm)
Time / min

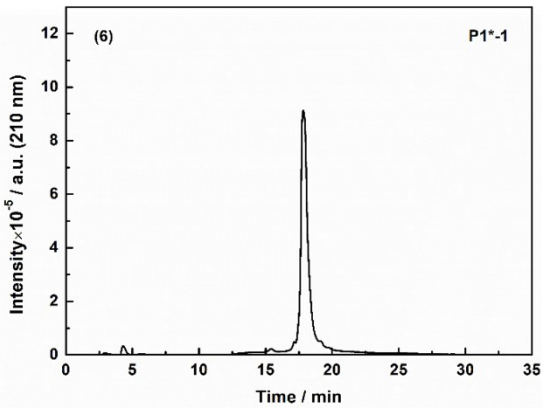
(6)
P1*-1
Intensity×10^{-5} / a.u. (210 nm)
Time / min

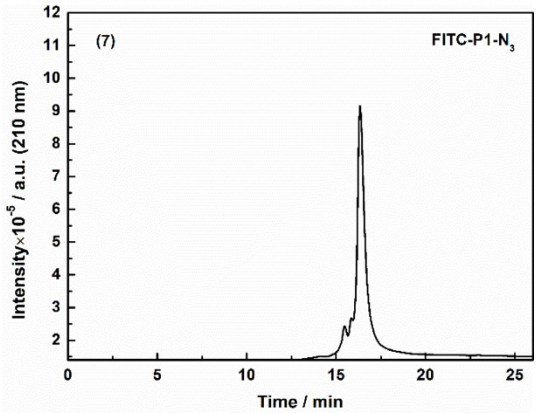
(7)
FITC-P1-N$_3$
Intensity×10^{-5} / a.u. (210 nm)
Time / min

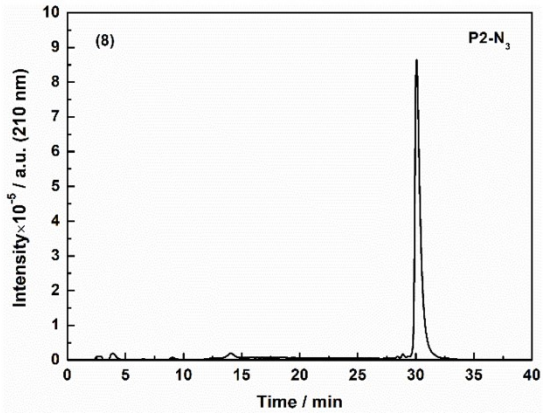
(8)
P2-N$_3$
Intensity×10^{-5} / a.u. (210 nm)
Time / min

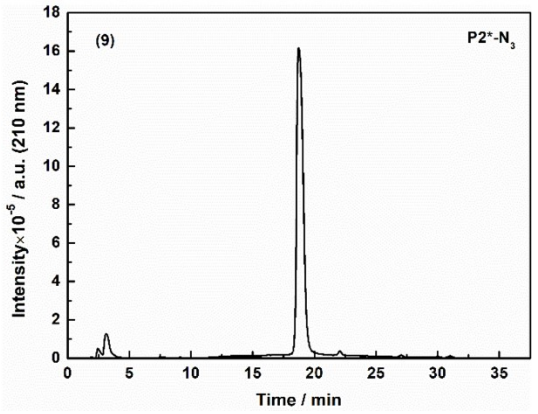
(9)
P2*-N$_3$
Intensity×10^{-5} / a.u. (210 nm)
Time / min

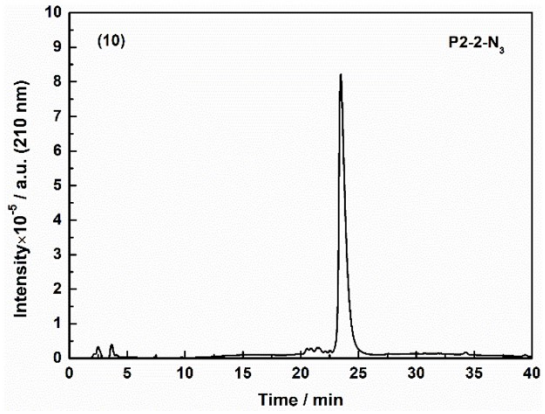
(10)
P2-2-N$_3$
Intensity×10^{-5} / a.u. (210 nm)
Time / min

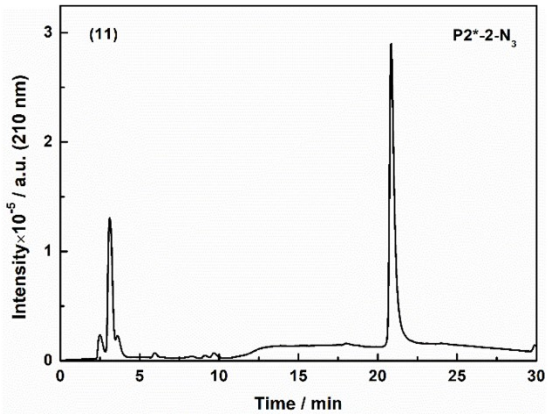
(11)
P2*-2-N$_3$
Intensity×10^{-5} / a.u. (210 nm)
Time / min

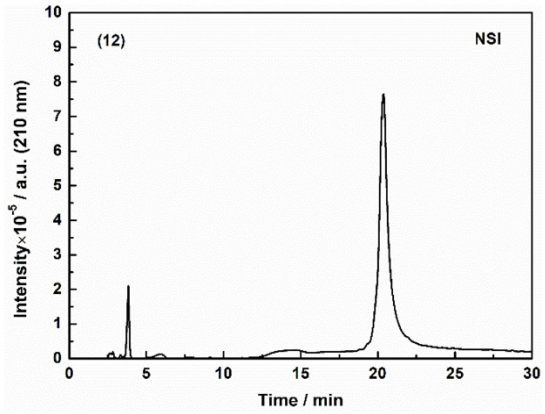
(12)
NSI
Intensity×10^{-5} / a.u. (210 nm)
Time / min

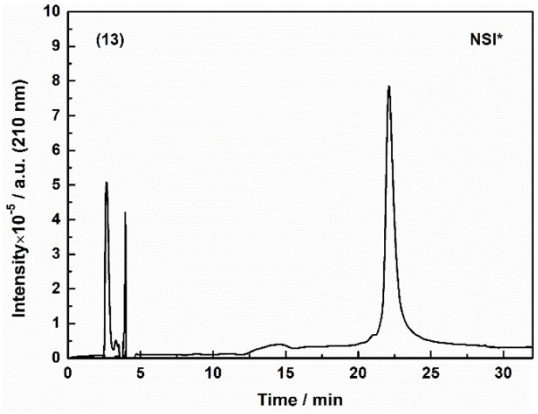
(13)
NSI*
Intensity×10⁻⁵ / a.u. (210 nm)
Time / min

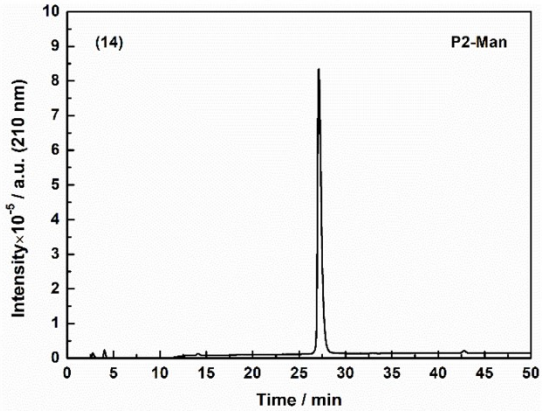
(14)
P2-Man
Intensity×10⁻⁵ / a.u. (210 nm)
Time / min

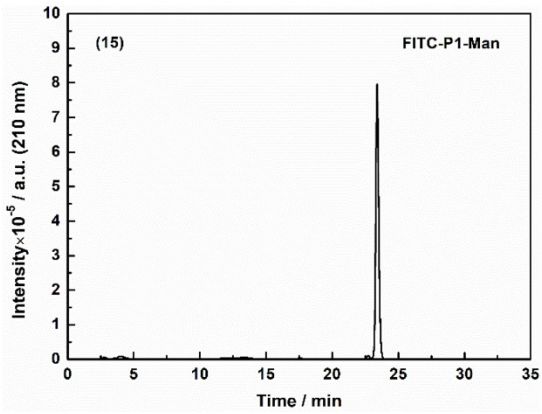
(15)
FITC-P1-Man
Intensity×10⁻⁵ / a.u. (210 nm)
Time / min

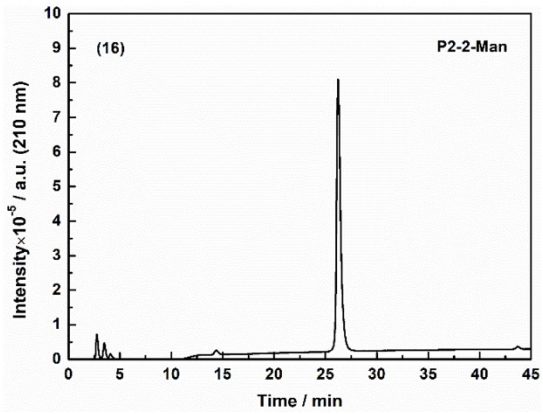
(16)
P2-2-Man
Intensity×10⁻⁵ / a.u. (210 nm)
Time / min

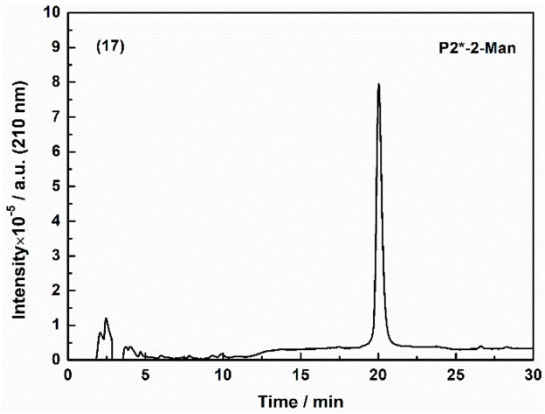
(17)
P2*-2-Man
Intensity×10⁻⁵ / a.u. (210 nm)
Time / min

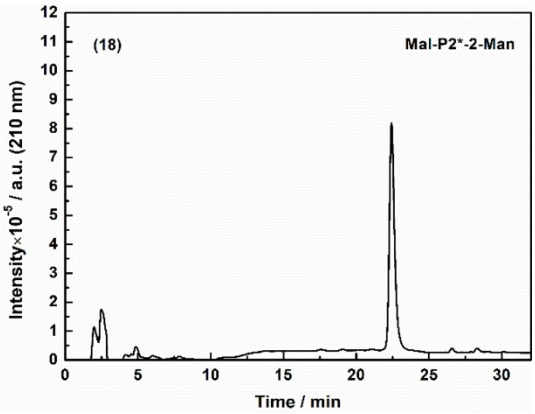
(18)
Mal-P2*-2-Man
Intensity×10⁻⁵ / a.u. (210 nm)
Time / min

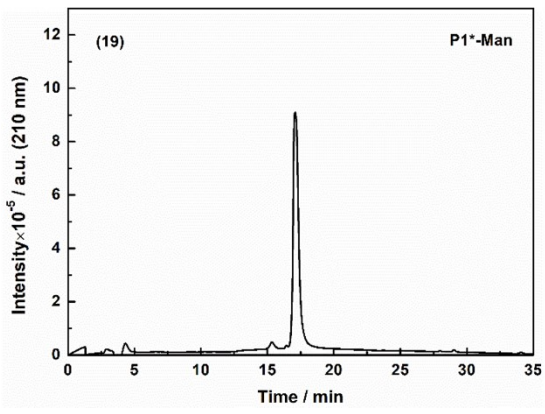
(19)
P1*-Man
Intensity×10⁻⁵ / a.u. (210 nm)
Time / min

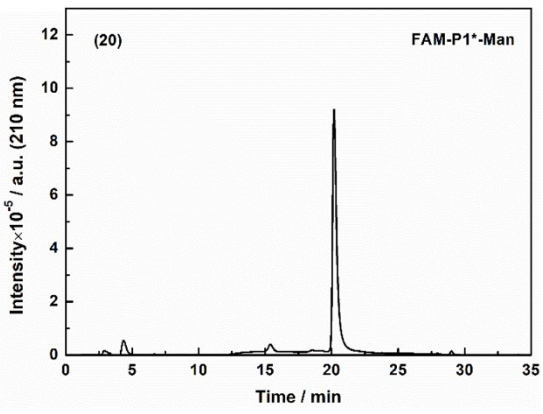
(20)
FAM-P1*-Man
Intensity×10⁻⁵ / a.u. (210 nm)
Time / min

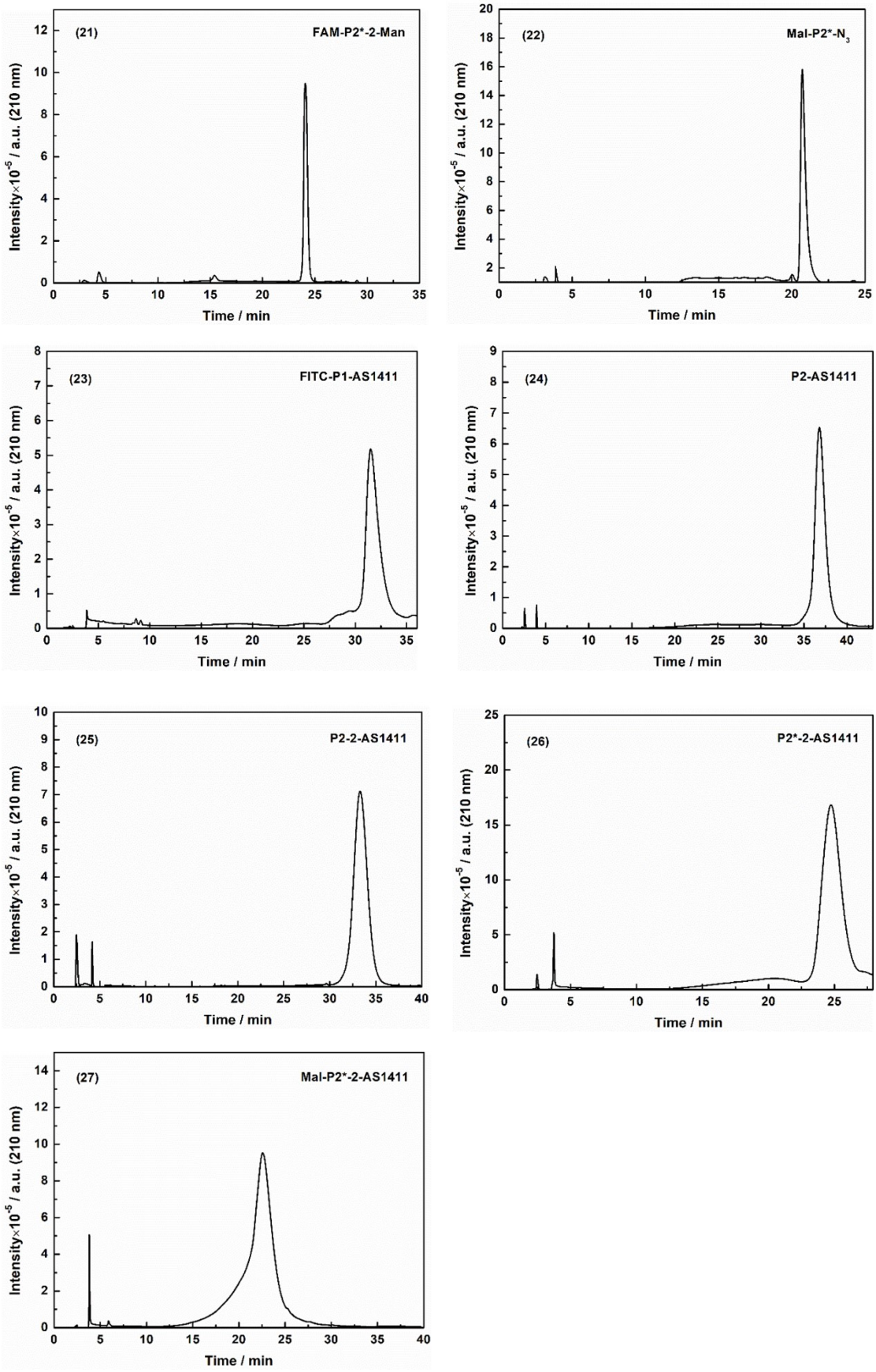

Figure S8 Analytical HPLC of **FITC-P1** (1); **P2-1** (2); **FITC-P1-1** (3); **P2-2** (4); **P2*-2** (5); **P1*-1** (6);**FITC-P1-N_3** (7); **P2-N_3** (8); **P2*-N_3** (9); **P2-2-N_3** (10); **P2*-2-N_3** (11); **NSI** (12); **NSI*** (13);

P2-Man (14); **FITC-P1-Man** (15); **P2-2-Man** (16); **P2*-2-Man** (17); **Mal-P2*-2-Man** (18); **P1*-Man** (19); **FAM-P1*-Man** (20); **FAM-P2*-2-Man** (21);**Mal-P2*-N_3** (22); **FITC-P1-AS1411** (23); **P2-AS1411** (24); **P2-2-AS1411** (25); **P2*-2-AS1411** (26); **Mal-P2*-2-AS1411** (27).

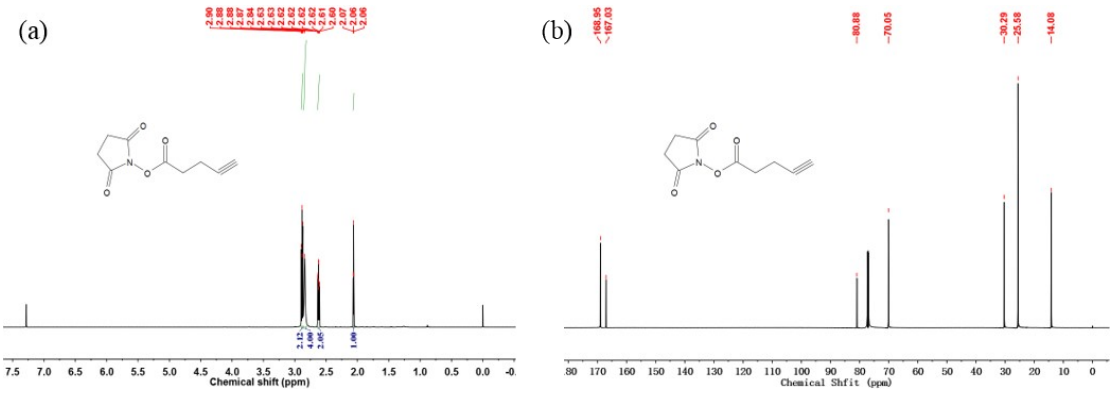

Figure S9 (a) ^{1}H NMR spectrum and (b) ^{13}C NMR spectrum of **NHS-III** in $CDCl_3$.

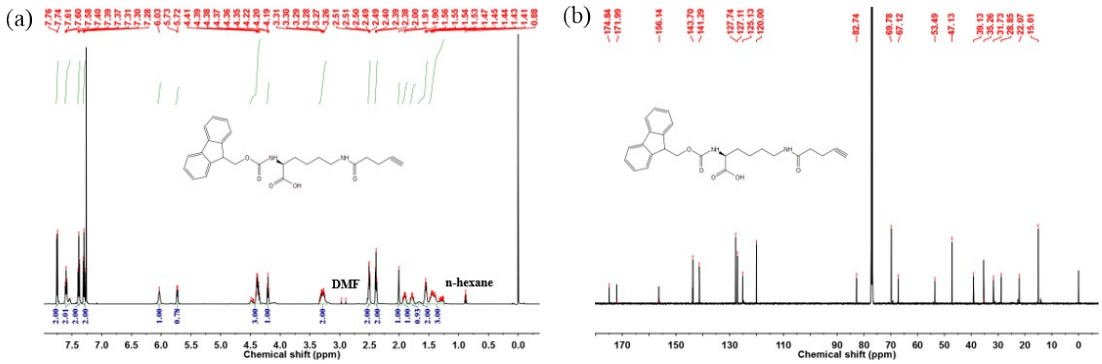

Figure S10 (a) ^{1}H NMR spectrum and (b) ^{13}C NMR spectrum of **Fmoc-Lys[*N*-4-Pentynoic acid]-OH** in $CDCl_3$.

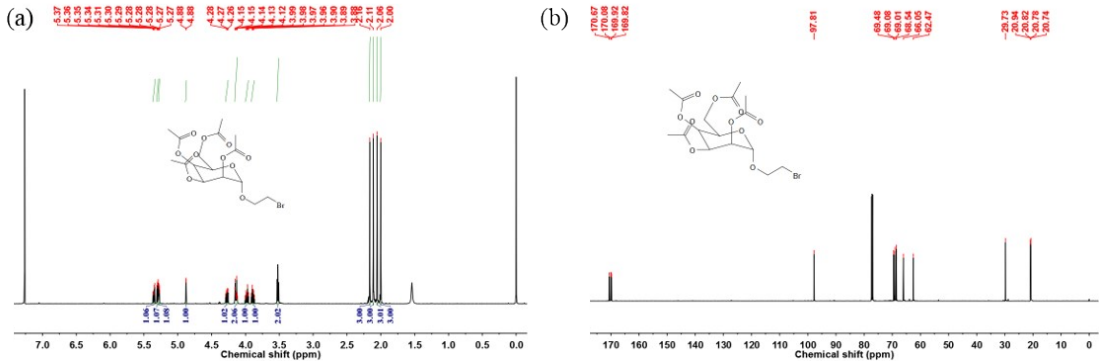

Figure S11 (a) ^{1}H NMR spectrum and (b) ^{13}C NMR spectrum of **M2** in $CDCl_3$.

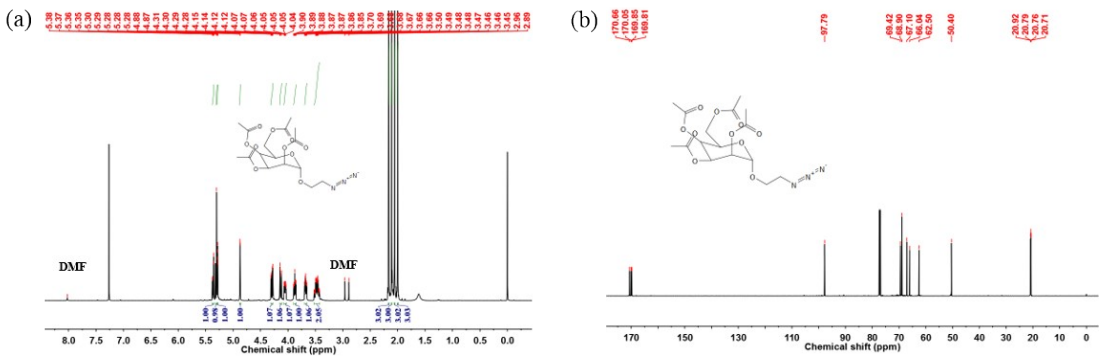

Figure S12 (a) ^{1}H NMR spectrum and (b) ^{13}C NMR spectrum of **M3** in $CDCl_3$.

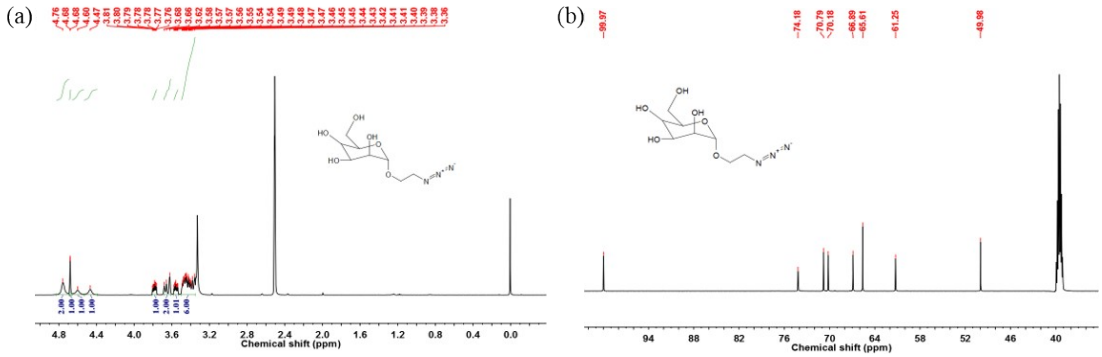

Figure S13 (a) ^{1}H NMR spectrum and (b) ^{13}C NMR spectrum of **M4** in DMSO-*d6*.

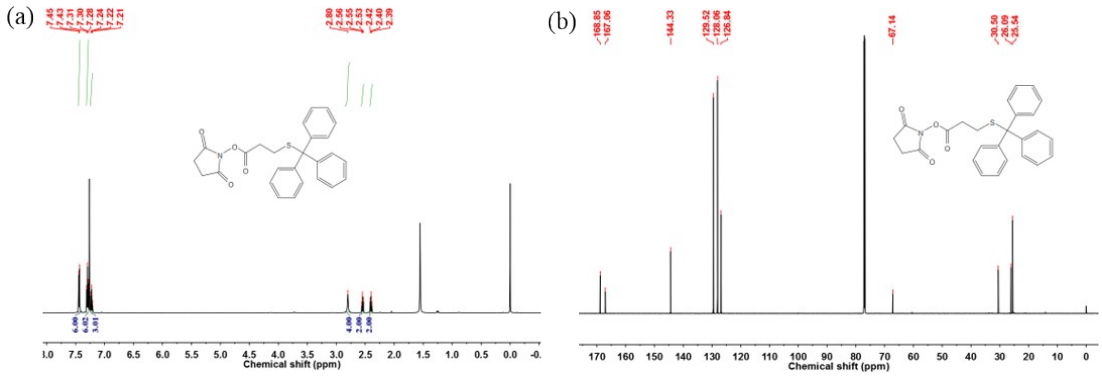

Figure S14 (a) ^{1}H NMR spectrum and (b) ^{13}C NMR spectrum of **NHS-Trt** in $CDCl_3$.

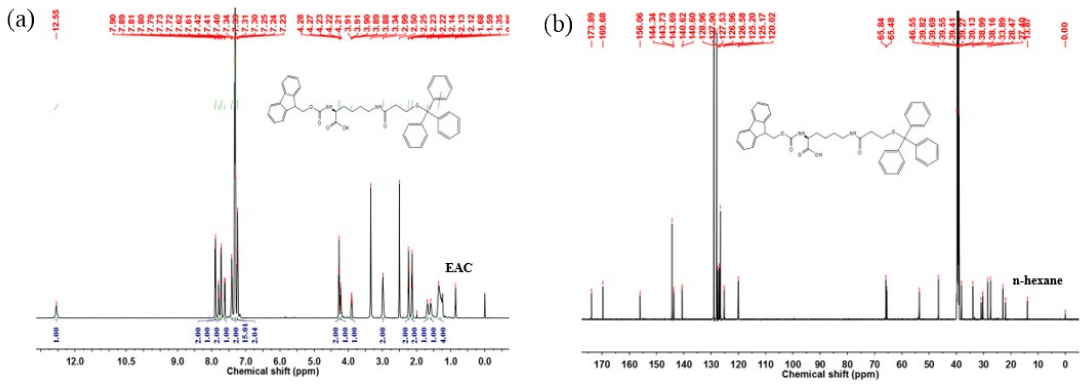

Figure S15 (a) ^{1}H NMR spectrum and (b) ^{13}C NMR spectrum of **Fmoc-Lys-S-Trt** in DMSO-*d6*.

6. References

1. M. Galibert, P. Dumy and D. Boturyn, Angew. Chem. Int. Ed., 2009, **121**, 2614-2617.

2. M. Galibert, O. Renaudet, P. Dumy and D. Boturyn. Angew. Chem. Int. Ed., 2011, **50**, 1901-1904.

3. L. Yin, Y. Chen, Z. Zhang, Q. Yin, N. Zheng and J. Cheng, Macromol. Rapid Commun., 2015, **36**, 483-489.